www.chuka.ac.ke library@chuka.ac.ke

2-D INVERSION OF GRAVITY DATA OF NYABISAWA-BUGUMBE AREA OF MIGORI GREENSTONE BELT, KENYA

Odek, A.[1] and Githiri, J.[2]
[1]Physical Sciences Department, Chuka University, P. O. Box 109-60400, Chuka
[2]Physics Department, Jomo Kenyatta University of Agriculture and Technology, P. O. Box 62000-00200, Nairobi aodek@chuka.ac.ke

Citation: Odek, A. and Githiri, J. (2017). 2-D Inversion of Gravity Data of Nyabisawa-Bugumbe Area of Migori Greenstone Belt, Kenya. In: Isutsa, D.K. and Githae, E.W. *Proceedings of the Third Chuka University International Research Conference held in Chuka University, Chuka, Kenya from 26th to 28th October, 2016. 129-137 pp.*

ABSTRACT
With the continuous extraction of minerals in Migori greenstone belt exploration is currently evolving from surface based exploration to subsurface exploration. This necessitates a good understanding of the geophysical features in the subsurface which are likely to have a direct bearing on the distribution of minerals. In this study, a 2-D litho-prediction model of Nyabisawa-Bugumbe area was developed from geologically constrained inversion of gravity field data. The measured gravity field data were subjected to cleaning process to remove perturbations which were not of geophysical interest, and later enhanced by removing long wavelength anomalies which are as a result of regional trend. The density variations were then inverted for the geometrical parameters of the model. Gravity high trending NW-SE around Nyabisawa, Kirengo towards Nyambeche was delineated. The gravity high is bounded by two major faults along rivers Migori and Munyu. Integrating the 2-D inversion of gravity data and the geology of the area, the gravity field perturbation is associated with banded iron formations.

Keywords: *Gravity, Anomalies, Migori Greenstone belt, Inversion, Minerals*

INTRODUCTION
Geological and Tectonic Setting
Migori greenstone belt runs west-northwest to east-southeast between Lake Victoria and the Great Rift Valley. The belt is squeezed between the diapiric migori granite batholith to the south and a felsic volcanic succession to the north. The structure of the Migori greenstone belt appears to reflect diapiric movements of the migori Granite batholith. The geology of the area consists of Archean greenstone belt that surrounds Lake Victoria. The Archean rocks in this area are principally of the Nyanzian system, the Kavirondian system and the post-Kavirondian granites that surround Lake Victoria (Shackleton, 1946).

The history of gold mining in this area, especially the history of Macalder mine, situated to the north-west of Migori town indicates the potential this area has for mineral production. In the vicinity of Macalder mine, gold occurs mostly in concordant quartz veins, some of which crop out and are worked

by artisanal miners as shallow opencast workings (Ngira exploration works, 2009). An explorer may need to know that systematic exploration is usually based on some conception of general or generic setting. In this case an ability to define host structures or units as well as vein location and orientations, coupled with the facility to discriminate mineralized from unmineralized terrain is required.

Gravity Technique

Gravity survey method can provide comprehensive structural, genetic and target evaluation and achieve site discrimination in terms of potential economic deposits (Leaman, 1992). Gravity data is acquired with the goal of determining distributions of density. This physical property can be interpreted in terms of lithology and/ or geological processes and their geometric distributions can help delineate geological structures and used as an aid to determine mineralization and subsequent drilling target (Philips et al., 2010). Because gold, which is one of the suspected mineral is typically associated with small scale structural features, dense, good-quality data and sharp positioning are important when searching an ore body (Airo and Mertanen, 2007).

Once data is obtained from gravity survey, variations in the earth's gravitational field which did not result from the differences of density in the underlying rocks were corrected. Drift correction was done by having a base station which was preoccupied periodically in the day. A drift curve was plotted and readings made in other stations assumed to have a linear drift as fitted base readings. Using the drift rate each reading was corrected to what it would have read if there were no drift.

Gravity varies with latitude because of the non-spherical shape of the earth, with polar radius shorter than equatorial radius. The theoretical value of gravity ($g\phi$) at given latitude (ϕ) is calculated using gravity formula:

$$g_{\emptyset} = 9.7803267714\,1 + 0.00193185138639 sin^2\emptyset / \sqrt{1 - 0.00669437999013 sin^2\emptyset}\ \mathrm{ms}^{-2} \ldots \quad 1.1$$

and it was subtracted from or added to the measured value to isolate latitude effect. As one moves away from the center of the earth, gravity decreases, the rate of decrease can be deduced by assuming spherical earth. From

$$g = GM/r^2 \quad 1.2$$

$$\delta g/\delta r = -2\,g/r = -0.3086\Delta h \quad 1.3$$

Where g is gravity, G is the universal gravity constant, r is the distance from Centre of the earth, M is the mass of the earth and h is the altitude. If the site is above the reference point, free air correction is added to the observed gravity value. If the site is below the reference point, free air correction is subtracted from the observed gravity value. Bouguer correction ($g=2\pi G\rho\Delta hg$) where ρ is the average crustal density, was done to remove the effect of attraction of a slab of rock present between the observation point and the datum. Terrain correction was also done to remove the effect of a hill or a valley at the vicinity of a station, which ultimately reduces the gravity value.

For gravity model, we shall consider an infinite long linear mass distribution with mass m per unit length extending horizontally along the y-axis at depth z. The contribution $d(\Delta g_z)$ to the vertical gravity anomaly Δg_z at a point on the x-axis due to a small element of length dy is:

$$d(\Delta g_z) = G\,m dy \sin\theta / r^2 = Gmz dy / r^3 \quad 1.4$$

$$\Delta g_z = Gmz \int_{-\infty}^{\infty} dy/r^3 = Gmz \int_{-\infty}^{\infty} dy/(u^2 + y^2)^{3/2} \quad 1.5$$

Where $u^2 = x^2 + z^2$ the integration is simplified by changing variables so that

$y = u\tan\varphi$,

$dy = u\sec^2\varphi d\varphi$ and $(u^2 + y^2)^{3/2} = u^3\sec^3\varphi$

This gives

$$\Delta g_z = Gmz/u^2 \int_{-\pi/2}^{\pi/2} \cos\varphi d\varphi \quad 1.6$$

which, after evaluation gives

$$\Delta g_z = 2Gmz/(u^2 + x^2) \quad \text{.....1.7}$$

Study Area

Gravity data was collected from 200 stations established over an area of 100 km^2 bounded by the latitudes 34˚25'E -34˚30'E and longitudes 1˚04'S – 1˚10'S in Nyabisawa-Bugumbe area of Migori Greenstone belt, with station and profile spacing of 300 m and 1 km respectively. Relative gravity measurements were taken using Worden gravity meter model prospect 410. All the gravity corrections were made for the effects which are not of direct geological interest, which includes correction for instrumental drift, free air, latitude, Bouger slab and terrain, the complete Bouger anomaly should contain information about the subsurface density alone. A contour map of the Bouger anomaly Figure 2.2 gives a good impression of subsurface density. The interpretation of gravity data involved identifying the anomalies from the Bouger anomaly map, selecting profiles across the anomalies as shown in the Figure and subjecting the profiles to both Euler deconvolution and Forward modeling.

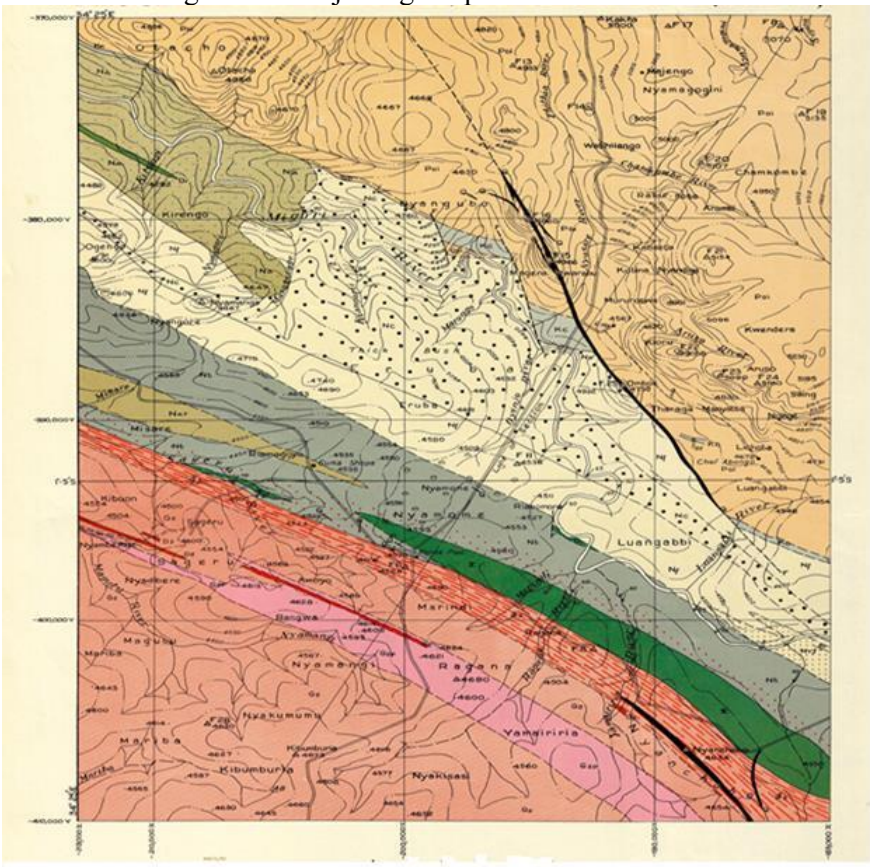

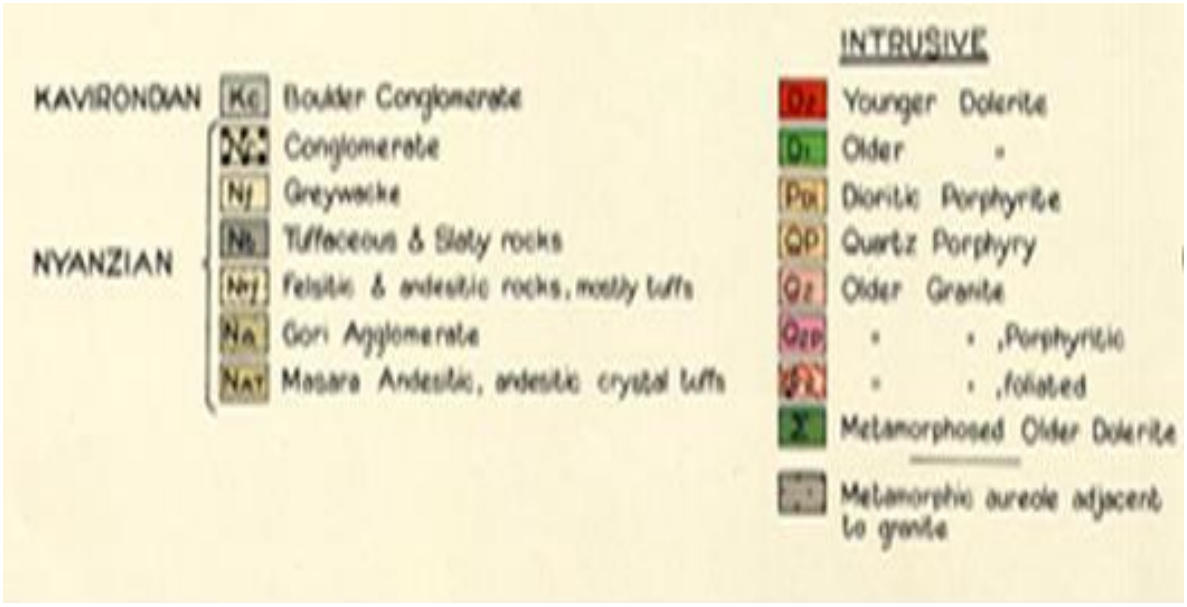

Figure 1.1: Local geology of Migori greenstone belt (Shackleton, 1946)

Theory

Euler Deconvolution aids the interpretation of gravity field. It involves determination of the position of the causative body based on an analysis of the gravity field and the gradients of that field and some constraint on the geometry of the body Zhang et al. (2000). The quality of the depth estimation depends mostly on the choice of the proper structural index which is a function of the geometry of the causative bodies and adequate sampling of the data Williams et al. (2005).

Figure 2.1: Location of Migori

Euler Deconvolution

It is based on the Euler equation of homogeneity:

$$(x-x_o)T_{zx}+(y-y_o)T_{zy}+(z-z_o)T_{zz}=n(B_z-T_z) \quad \text{.....1}$$

for the gravity anomaly vertical component T_z of a body having a homogeneous gravity field, (x_o, y_o, z_o) are the unknown co-ordinates of the source body centre to be estimated. (x, y, z) are the known co-ordinates of the observation points of the gravity and gradients. The values T_{zx}, T_{zy}, T_{zz} are the measured gradients along the x-,y- and z-directions, n is the structural index and B_z is the regional value of the gravity to be estimated. In 2-D this equation reduces to:

$$(x - x_o)T_{zx} + (z - z_o)T_{zz} = n(B_z - T_z) \quad \text{.....2}$$

There are three unknown parameters (x_o,z_o and B_z). In this study, a structural index of 0.5 was adopted since it gives the most accurate depth estimates for gravity data where the typical source structures are finite-offset (Williams et al., 2005). With selected window, there are n data points available to solve the three unknown parameters. When n>3, these parameters can be estimated (Zhang and Sideris, 1996).

Interpretation of Euler Solutions

In this study the results were generated using Euler 1.0 software after Cooper (2004).

Figures 3(a), 3(b) and 3(c) below, shows the vertical and horizontal gradients of the gravity field and 2-D Euler solutions for profiles AA', BB' and CC'. The solutions cluster well at a shallow depth estimated to be between 50 m to 750 m. The depth of these high gravity causative bodies under profiles AA', BB' and CC' coincide well with the geology of the study area which reveals stripes of banded iron formation suspected to host majorly gold mineral. The scattered solutions which are not well constrained (spurious) were rejected during the interpretation.

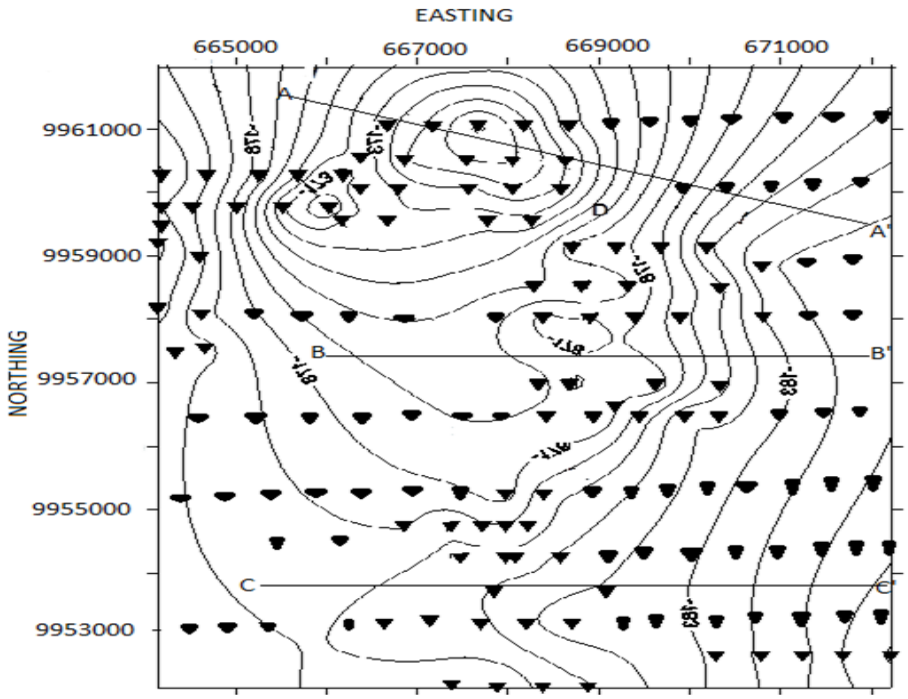

Figure 2.2: Complete Bouguer anomaly contour map.

Conventional Euler deconvolution produces spray of solutions, within which the correct answer for each discrete body needs to be found. Weighted least squares minimize the errors in the solution for best fit and also give local error estimates. In order to distinguish more reliable solutions from spurious ones, some of the discrimination techniques proposed by Desmond et al. (2004) were used, these includes; analysis of the clustering of solutions, rejection of bodies that have inadmissible structural index, low pass filtering of the data to constrain the frequency content and rejection of solutions based on reliability.

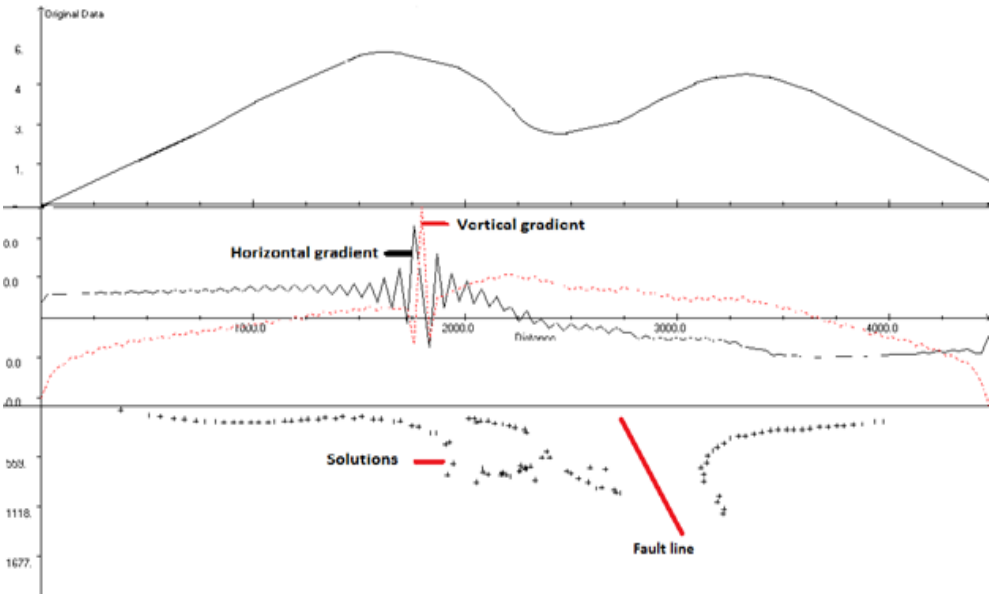

Figure 3(a): Euler Deconvolution along profile AA'.

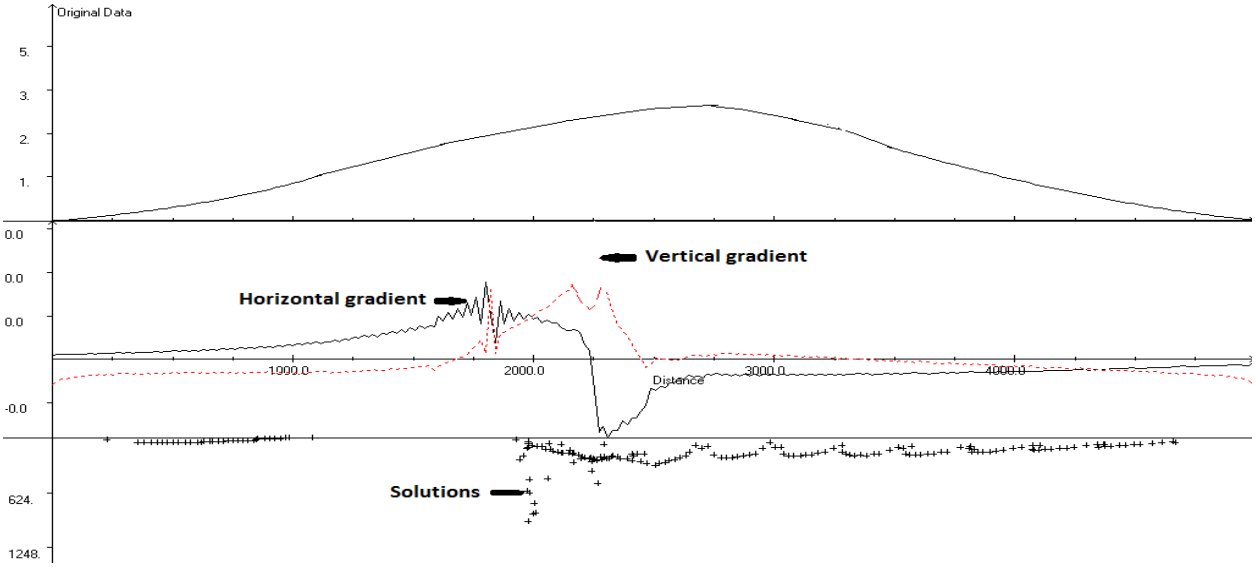

Figure 3(b): Euler Deconvolution along profile BB'.

Forward modelling

Theory

This interpretation technique is applied where the shapes and depths of anomaly sources are important, it involves preparation of gravity field models of a subsurface using all available geological information, it is then compared with the field actually observed (Parasnis, 1986). The model is then modified, within the limits set by the geological constraints, until a satisfactory level of agreement is reached between calculation and observation. This process was done using the grav2DC software developed by Talwani et al (1964). The final model is not, of course, necessarily correct, and since other mass distributions will exist that satisfy all the conditions, but it is at least a possible solution. In this study the modifications to the model was performed interactively on a computer screen which shows both the model and the gravity data. Two-dimensional approximations were used in which the geology is assumed not to vary at right angles to the line of profile and section and is generally adequate provided

that the strike length of the anomaly is at least three times as great as the cross-strike width (Barker and Wohlenberg, 1971). The start up model depth was obtained from the direct interpretation and Euler deconvolution solutions.

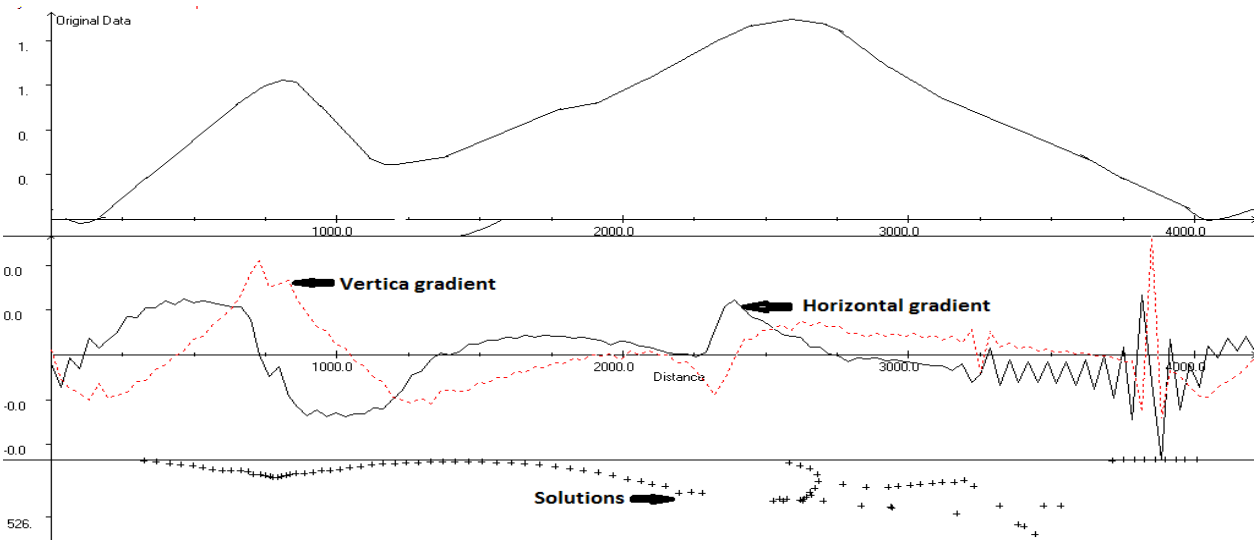

Figure 3(c): Euler Deconvolution along profile CC'.

2-D Forward modelling interpretations

Profile AA' is used to model the gravity high anomaly centered at grid co-ordinates (668000, 9954500). The result of the forward modeling shows a dense structure with the maximum depth to the top as 150 m, density contrast 0.1832 g/cm^3 and a width of 3.321 km. Figure 4(a) shows the fit between the computed gravity anomaly curve and the observed anomaly along profile AA'. Similarly, Profiles BB' is used to model gravity high anomaly centered at grid co-ordinates (666000, 9955200). The best fit is obtained at a depth of about 200 m, density contrast 0.3908 g/cm^3 and a width of 604 m. Profile CC' cuts across a series of gravity high anomalies. The modeled structure is a dense body of density contrast approximately 0.1035 g/cm^3 at a depth range about 50 m to 540 m and a width of 2.674 km. Figure 4(c) displays the fit between the anomaly curve as a result of the calculated body and the observed anomaly curve.

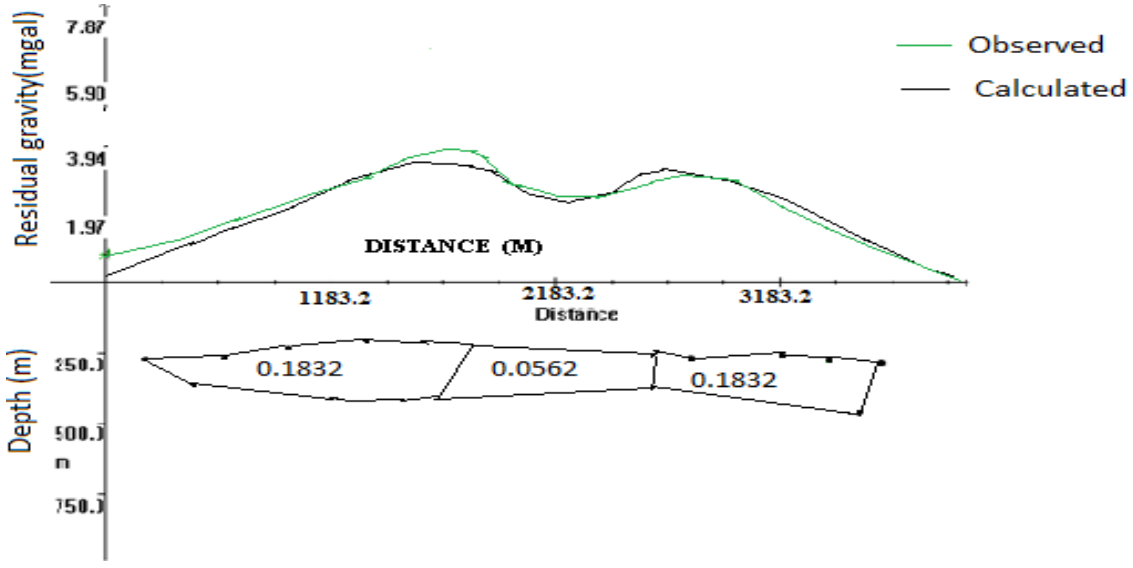

Figure 4(a): Observed, calculated anomaly and forward model for 2-D body along profile AA'.

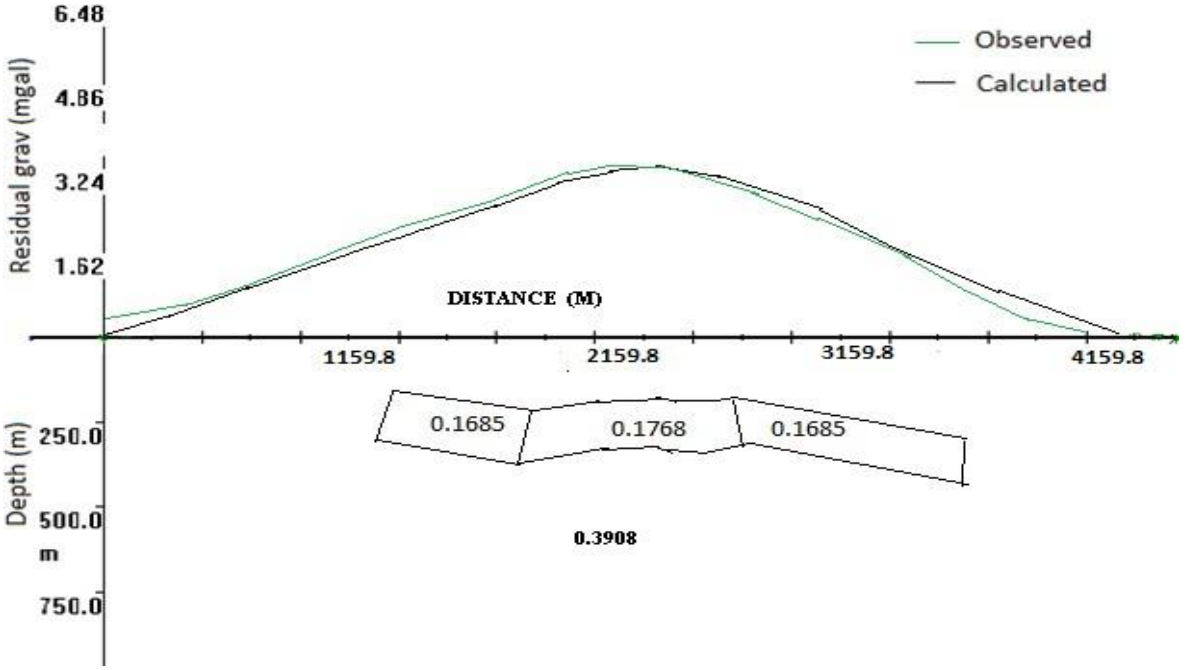

Figure 4(b): Observed, calculated anomaly and forward model for 2-D body along profile BB'.

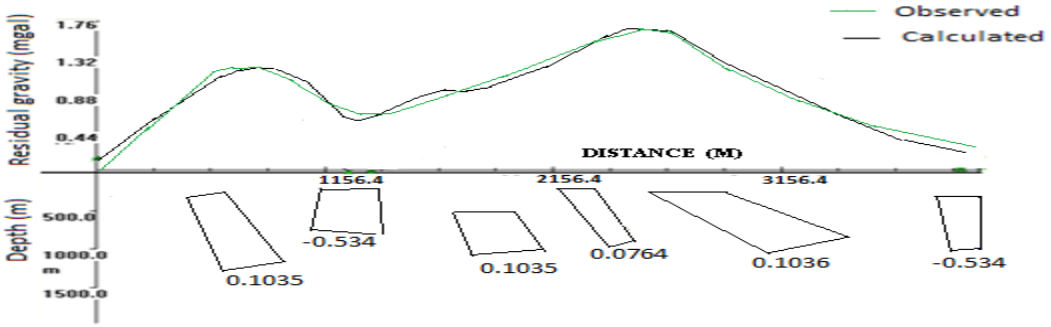

Figure 4(c): Observed, calculated anomaly and forward model for 2-D body along profile CC'.

CONCLUSION

The result of this study shows that the Northern part of Nyabisawa-Bugumbe area of Migori Greenstone belt consist of gravity highs which can be associated with relatively high density bodies compared to the surrounding rocks. An integration of this study with the geological report of the study area shows the possibility of the banded iron formations which occasionally act as a host to other minerals like gold being the cause of the high density. These dense structures have been modelled to be at a depth of about 50-750 m from the surface on the northern part of the study area.

ACKNOWLEDGEMENT

We wish to acknowledge Chuka University and Jomo Kenyatta University, Physics Departments for availing the geophysical survey instruments. We also acknowledge the Department of Mines and Geology for availing the geological report of Migori Greenstone belt.

REFERENCES

Airo M.L. and Mertanen S. (2007). Magnetic signatures related to Orogenic gold mineralization, Central Lapland greenstone belt Finland. Geological survey of Finland. Finland.

Baker, B.H. and Wohlenberg, J. (1971). "Structure and evolution of the Kenyan Rift Valley." Nature, 229:538-542.

Cooper, G. 2004. Euler deconvolution applied to potential field gradients. Exploration Geophysics, 35:165-170.
Desmond F.G., Philip M. and Alan R. (2004). New discrimination techniques for Euler deconvolution. Reid Geophysics, University of Leeds, UK.
Leaman D.E. (1992). Gold exploration and use of magnetic method in Northern Tasmania. Bulletin Geological Survey. Tasmania.70: 149-160.
Ngira Exploration Works Ltd, (2009). A geological overview of the licence area for Ngira exploration works Ltd. Ngira.
Parasnis D.S. (1986) Principles of Applied Geophysics. Chapman and Hall, U.S.A. 61-103
Philips N., Nguyen T.N.H., Thomson V., Oldenburg D., Kowalezyk P. (2010). 3D inversion modelling, integration and visualization of airborne gravity, magnetic and electromagnetic data Advanced Geophysical Interpretation centre, Vancouver, B.C. Canada.
Shackleton R.M. (1946). Geology of Migori Gold belt and adjoining areas. Geological survey of Kenya, Mining and Geological Department Kenya, Rept. 10: 60.
Talwani, M. and Heirtzler, J.R. (1964). "Computation of magnetic anomalies caused by two dimensional structures of arbitrary shape, in Computers in the mineral industries," part 1: Stanford University publications, Geol. Sciences, 9: 464-480.
Telford W., Geldart L., Sheriff R. and Keys D. 1976. Applied Geophysics. CUP, 860.
Williams S.E., Fairhead J.D., and Flanagan G. (2005). "Comparison of grid Euler deconvolution with and without 2D constraints using a realistic 3D magnetic basement model." Geophysics, 70, 13-21.
Zhang C. and Sideris M.G. (1996). Ocean gravity by analytical inversion of Hotines formula, Marine geodesy 9: 115-135.

******